Bulletin of the Geological Society of Greece
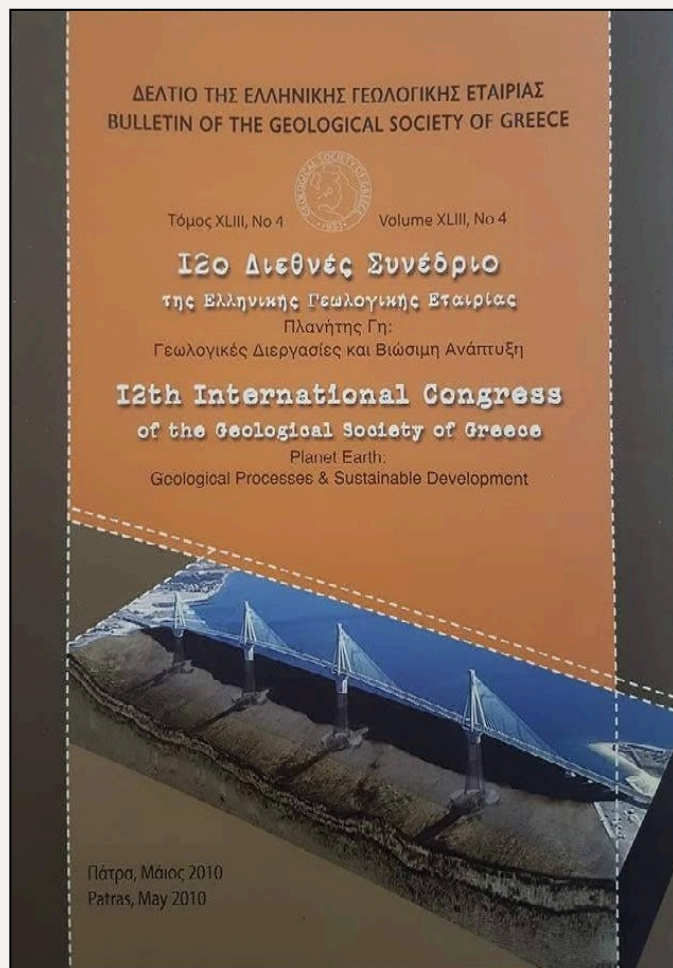
COMPILATION OF A UNIFIED AND HOMOGENEOUS AEROMAGNETIC MAP OF THE GREEK MAINLAND

Chailas S.	Department of Geophysics – Geothermy, National and Kapodistrian University of Athens
Tzanis A.	Department of Geophysics – Geothermy, National and Kapodistrian University of Athens
Kranis H.	Department of Dynamic, Applied and Tectonic Geology, National and Kapodistrian University of Athens
Karmis P.	Institute of Geology and Mineral Exploration, Geophysics Department

To cite this article:

COMPILATION OF A UNIFIED AND HOMOGENEOUS AEROMAGNETIC MAP OF THE GREEK MAINLAND

Chailas, S.[1], Tzanis, A.[1], Kranis, H.[2] and Karmis, P.[3]

[1] *Department of Geophysics – Geothermy, National and Kapodistrian University of Athens, Panepistimiopoli, 15784 Zografou, Greece; schailas@geol.uoa.gr; atzanis@geol.uoa.gr*

[2] *Department of Dynamic, Applied and Tectonic Geology, National and Kapodistrian University of Athens, Panepistimiopoli, 15784 Zografou, Greece; hkranis@geol.uoa.gr*

[3] *Institute of Geology and Mineral Exploration, Geophysics Department, Sp. Loui 1,Olympic Village, 13677 Acharnae – Athens, Greece, karmis@igme.gr*

Abstract

We present a unified and homogeneous digital aeromagnetic map of the Hellenic mainland, based on the 1:50,000 map series of IGME. These maps cover the areas A1, A2, B, C1, C2, C3, D1 compiled by Hunting Geology and Geophysics Ltd. and measured at nominal ground clearances (flight altitudes) 150m AGL, 150m AGL, 300m AGL, and 2300m AMSL respectively (part of C2 with 3000m AMSL). We also include the entire area of Northern Greece, measured by ABEM AB with nominal ground clearance 275±75m AGL. The original map sheets were digitally imaged, georeferenced, digitized along contour lines and interpolated onto regular 250΄250m grids. The unified aeromagnetic map was constructed by collating the mosaic of the resulting gridded data. Using upward/downward continuation techniques various homogeneous versions of the map, were compiled by referencing of the observed mosaic total magnetic field to a unique constant ground clearance or to a unique constant elevation above mean sea level. This is the first time there is a complete and unified image of the magnetic signature of the isopic zones and rock formations comprising the Hellenic mainland, with particular reference to the ophiolite suites, which provides additional insight into the Alpine and post-alpine tectonics of the area.

***Key words:** Greece, aeromagnetic map.*

1. Introduction

The scope of the work reported herein is very clear: To compile a unified and common-referenced aeromagnetic map of Greece, out of the fragmentary information existing in a multitude of 1:50000 scale maps produced by different contractors for the Institute of Geological and Mining Research (IGME).

The original aeromagnetic data set was acquired in two stages: In 1966, ABEM AB conducted a field campaign over Central/ Eastern Macedonia and West Thrace (the hatched area in Fig. 1). In 1977, Hunting Geology and Geophysics Ltd conducted a second campaign extending over West Macedonia, Thessaly, eastern Central Greece, and eastern Peloponnesus (Areas A, B, C and D in Fig. 1). Both contractors delivered the raw data in analogue or digital magnetic tape and the end product in 1:50000 scale contour maps compiled so, as to comply with the corresponding topographic

maps of the Hellenic Army Geographical Survey (HAGS) and the 1:50000 geological maps of IGME.

The "original" 1:50000 scale maps did not comprise a uniform set. Each contractor used different reduction and processing schemes, which resulted in significant inconsistencies at the boundaries between their respective survey areas. Moreover, ground clearance was different between sub-areas surveyed by the same contractor, so that their respective 1:50000 maps were not directly comparable (for details see below). In *several* occasions, when the boundary between two sub-areas surveyed with different ground clearances would straddle a single HAGS/IGME sheet, the *same* 1:50000 aeromagnetic map would be produced with *different* data and contouring schemes (for an example see Fig. 2); this would certainly hinder interpretation and often beget confusion to the novice or unfamiliar with the analysis of potential fields.

National or regional scale maps of commonly reduced and referenced aeromagnetic data for the entire Hellenic territory at different absolute elevations have not been systematically produced. In consequence, regional or spatially extended aeromagnetic anomalies could not be recognized and evaluated. Even local anomalies straddling the boundaries between two maps were discontinued and had to be reconstructed by the interested investigator. Finally, until recently, no information whatsoever existed in some digital form. The only hitherto known attempt to unify a significant subset of the aeromagnetic data and investigate aeromagnetic anomalies at large scales was that of Stampolidis (1999) who *reprocessed* the original flight line data collected by ABEM in Northern Greece.

Inasmuch aeromagnetic surveys aim at the detection of extended – regional scale anomalies and are best suited for strategic scale investigations, the aforementioned limitations and difficulties have hindered their utilization, to the point of leaving a valuable resource mostly unexploited and largely ignored. Herein, we attempt to remedy this situation by producing a unified aeromagnetic map of Greece for the first time and thus bring up an important piece of infrastructure and asset of pure and applied Earth-scientific research.

2. Data Sources

As mentioned above, the compilation of the unified and homogeneous aeromagnetic map of Greece is based on the 1:50,000 map series of IGME, produced by ABEM AB and Hunting Geology and Geophysics Ltd.

The ABEM maps (ABEM, 1967), were produced with measurements at a nominal constant ground clearance (GC) of 275±75m above ground level (AGL) i.e. in constant ground clearance mode. The direction of the flight lines (tracks) was NE-SW and the mean distance between them was about 1km. Connection (tie) lines for crossover adjustment of the data were also flown at NE-SW direction, with a mean distance of 10km.

Hunting Geology and Geophysics Ltd. has generally used a magnetic field measurement spacing of 200–250m and has flown on a NE-SW direction, but at different GC's and track densities depending on the topography. The data collection schemes are as follows (also see Fig. 1):

- Area A1 (Thessaloniki basin): Nominal GC 150m AGL at a nominal distance of 400m between tracks.
- Area B (Thermaikos Gulf): Nominal GC l 150m above mean sea level (AMSL) at a nominal distance of 400m.
- Area C1 (Paikon Mountain): Nominal GC 300m AGL at a nominal distance of 800m.
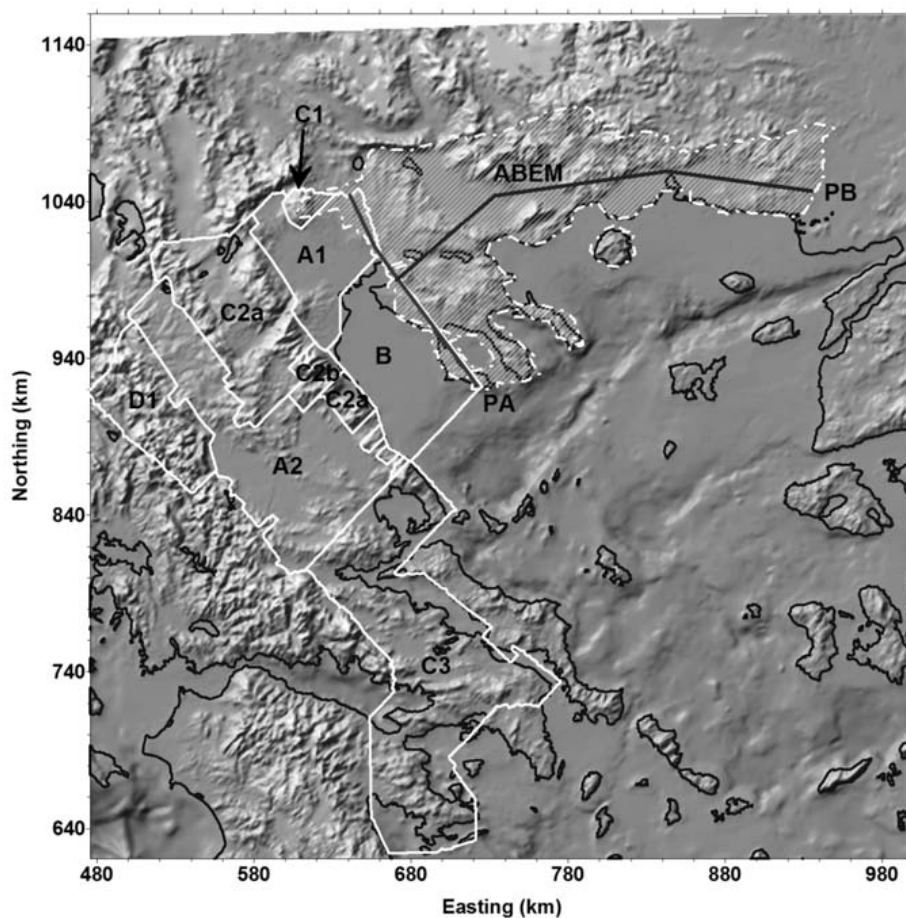
Fig. 1: Map showing the area coverage of the aeromagnetic data.

- Area C2a (the highlands between Thessaloniki and Thermaikos basins to the east and the Pindus Mt. chain to the west, including the Florina and Ptolemais basins): Nominal GC 300m AGL at a nominal distance 800m between tracks.
    - Exception is the area of Mt. Olympus, (area C2b) where the flight level was 3000m AMSL with the same nominal distance between lines.
- Area A2 (the Mesohellenic trough and the Karditsa and Larissa basins): Nominal GC was 150m AGL at a nominal distance of 400m.
- Area C3 (Eastern Central Greece): Nominal GC 300m AGL at a nominal distance of 800m.
- Area D1 (the Pindus Mt. chain): Nominal flight level was 2300m AMSL at a distance of 1000m between tracks.

In all cases, connection lines were flown at a NE-SW direction and a spacing of 10km. The IGRF correction was based on the IGRF model for the epoch 1977.3. A constant value of 150nT was added to the magnetic anomaly values prior to plotting the contour maps. It is probably worth noting that the original raw data set delivered by Hunting Ltd in magnetic tapes, has been irreversibly damaged and all that was left from this important survey are the 1:50000 contour maps.
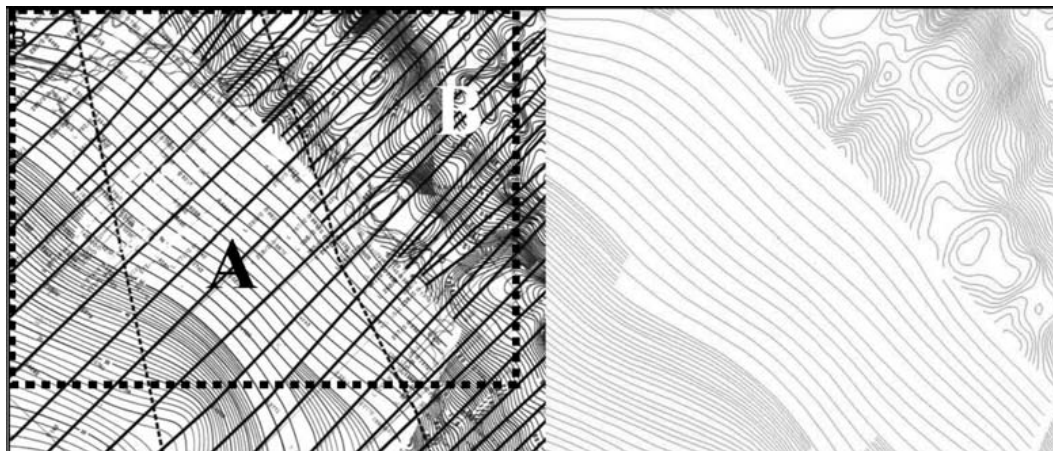
Fig. 2: Left: Part of the aeromagnetic map of sheet 'Kalampaka', scale 1:50.000. The continuous NE-SW lines indicate the primary flight lines and the dashed NW-SE lines the connecting (tie) lines. Area A was measured at a constant ground clearance of 2300m and flight line spacing of approx. 1000m Area B was measured at a cgc of 150m, with flight line spacing 400m. The change in the detail and the appearance of local anomalies is evident. Right: The digitized contour lines for the inset rectangle faithfully reproduce the original map.

3. Digitization and Gridding Procedure

The original 1:50000 map sheets were initially converted to a high resolution raster image format (typically TIFF). The contour lines were then digitized to vector form (image coordinates) with sufficiently high sampling densities, so as to faithfully reproduce the original image. Fig. 2 shows a part of an original map in raster format (left) and the resulting plot of the digitized contours. The boundaries between neighbouring areas with different flight parameters were also digitized. Using the corners of the map sheets as control points, the map were georeferenced and the image coordinates were transformed to Cartesian coordinates in the UTM projection. The digitized contour lines were subsequently stored in area-files according to the data collection schemes (flight line characteristics) detailed of Section 2. The area files were then interpolated to a regular grid, using a grid spacing of 250m.

The selection of the grid spacing was an exercise in optimal compromise and deserves some attention. First, let it be noted that the magnetic measurements along flight lines were taken at intervals of the order of 200m and certainly £250m. In consequence:

1. This interval is directly comparable to the flight line spacing of 300m for areas measured at 150m AGL. When projected to a direction perpendicular to a flight track, the distance is approx. 353m, longer than the nominal distance between lines. This ensures the faithful reproduction of the local aeromagnetic anomalies.

2. For lines flown 800 and 1000m apart (areas measured at 300m and 275m AGL respectively), the projection at a direction perpendicular to the line is respectively 44% and 35% the distance between flight tracks. This is just sufficient to ensure reproduction of aeromagnetic anomalies with minimal noise (interpolation artifacts) at short wavenumbers.

3. For track lines spaced 1000m and 800m apart and flight levels 2300m and 3000m respectively, the measured field is already smooth enough, to ensure that short wavenumber artifacts will not be introduced during interpolation.

On collating the mosaic of the resulting gridded areas to build a first draft of the aeromagnetic map,
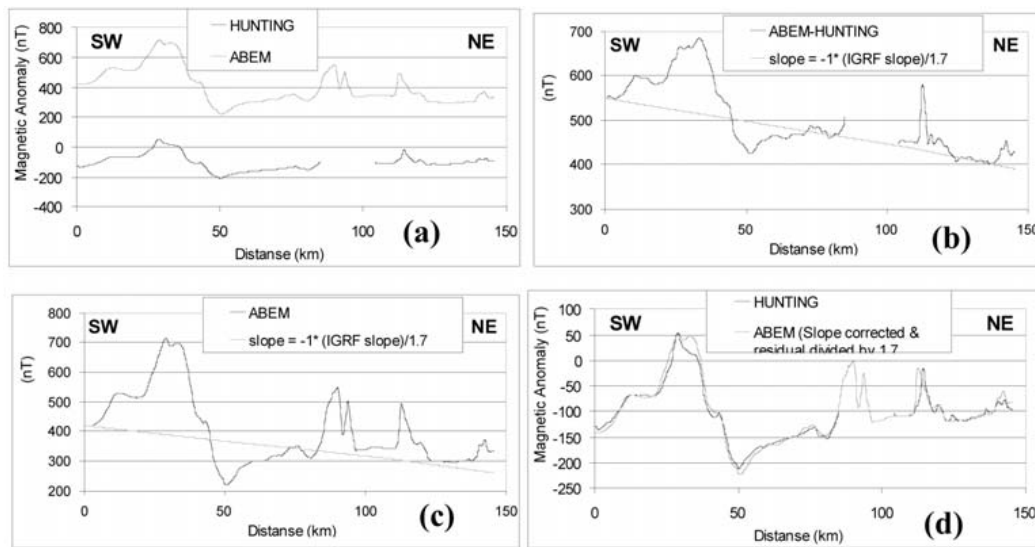
Fig. 3: (a) The total magnetic field along the profile PA in the overlapping region of the ABEM and Hunting survey areas (see Fig. 1). (b) Plot of the difference between the profiles of Fig. 3a. The trend line was calculated as a scaled function of the IGRF slope along the profile. (c) Plot of the ABEM profile with similarly calculated trend line. (d) The profiles of Fig. 3a after reduction of the ABEM data for the trend and scaling for the 1:1.7 distortion factor (see text for details).

we observed an offset of ~450nT (mean datum value) between the Hunting and ABEM data sets in the region where areas A and C1 C2 overlap (Fig. 1 and Fig. 3b), which could not be attributed to the ~125m difference in the flight level: although ABEM was flying higher than Hunting, their contoured magnetic field values were already higher than those of Hunting! In order to investigate the reasons behind the difference of the two data sets, a SW-NE profile was sliced from both data sets across the overlapping region (profile PA in Fig. 1). As can be seen in Fig. 3a, the same local magnetic features are present in both profiles, but the ABEM data is not only upwards offset, but also appears to be vertically exaggerated! Subtraction of Hunting's values from ABEM's profile revealed the existence of a regional trend in the differences (Fig. 3b). Comparing these differences with the slope of the IGRF model for the epoch 1966.5, we found that the trend line is actually a scaled version of the IGRF with a ratio equal to 1:1.7. We have also found that this trend can be *exclusively* attributed to the ABEM data (Fig. 3c). After subtracting the trend from the ABEM profile and scaling the residual curve, the Hunting and ABEM profiles have practically coincided (Fig 3d). The discrepancy between the Hunting and ABEM maps can therefore be attributed to a distorted (erroneous) IGRF correction of the ABEM data.

The first draft of the "unified" Greek aeromagnetic map was constructed by collating the mosaic of the gridded areas, after correcting the ABEM data for the offset of 450nT and the Hunting data for the constant of 150nT added prior to plotting. The result is shown in Fig. 4. It is immediately apparent that the boundaries between different areas are discontinuous and the texture of the map inhomogeneous and different between different survey areas, as a result of the differences in the data acquisition procedures.

An additional observation is that the ABEM data exhibit a persistent eastward downward slope. The comparison of the map of Fig. 4 with the aeromagnetic map of Turkey (Akin, 2007; comparison is not presented herein) has also shown differences of the order of 200nT at the boundaries. Given the analysis presented above for the differences between the Hunting and ABEM data, it would appear
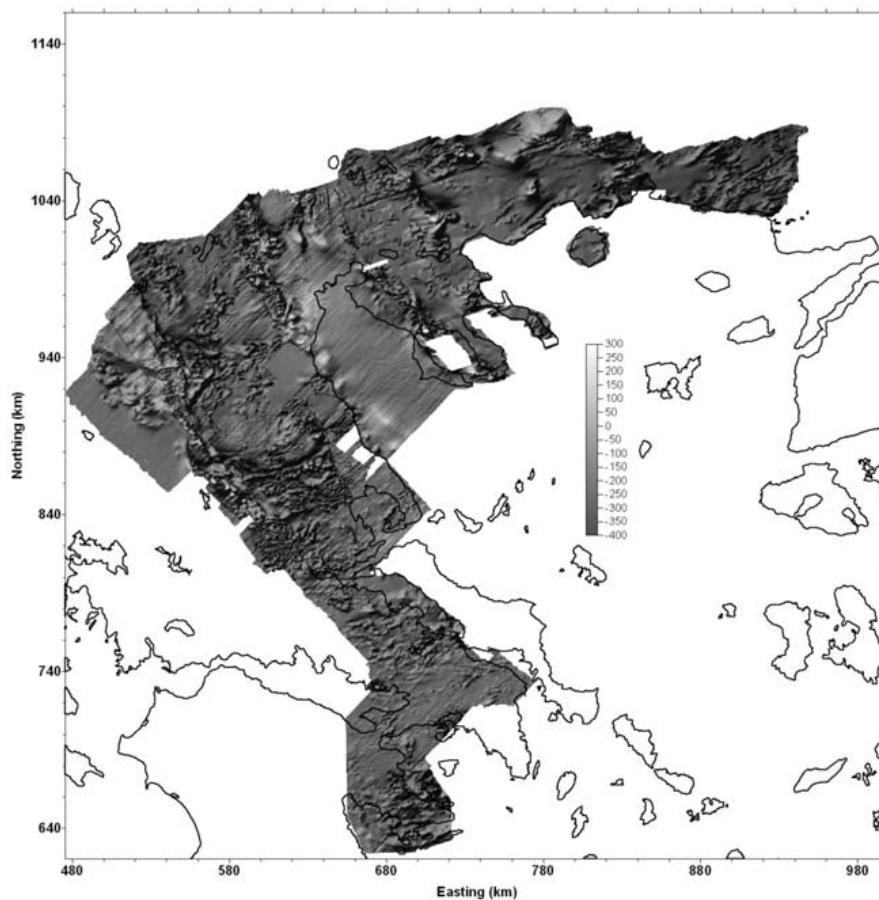
Fig. 4: The mosaic aeromagnetic map produced by digitizing the 1:50.000 scale aeromagnetic maps by Hunting Ltd and ABEM AB. A constant value of 450nT has been subtracted from the ABEM data and a constant value of 150nT from the Hunting data; the latter has been arbitrarily added prior to plotting. The obvious discontinuities across area boundaries are due to the different data collection schemes (see Section 2). The eastward downward slope observed in the ABEM data is due to a distorted IGRF correction (see text for details).

that the same distorted IGRF correction is to blame for the downward slope, as well as for the discrepancy between the Greek and Turkish data. In order to confirm the effect, we have constructed a W-E profile along the ABEM area, as shown in Fig. 1 (profile PB). The profile is plotted in Fig. 5a, together with the trend line calculated as a scaled version of the IGRF model for the epoch 1966.5, in the same manner as per Fig. 3c. Fig. 4d shows the same profile before (continuous black line) and after de-trending and re-scaling (continuous grey line). It is apparent that the original and corrected profiles exhibit a difference of approx. 200 nT at the east end of the profile, approximately the same as the difference observed between the Greek and Turkish data. It is therefore confirmed that the aeromagnetic contour maps delivered by ABEM are distorted. The actual reason for this distortion is still not known, but the previous analysis indicates, either incorrect reduction of the data, or a recorder calibration error. What is important however is that the effect has been recognized and may be reversed using the procedure described above.

The map of Fig. 4 is certainly unified, inasmuch as this is the first time that the mosaic of the different aeromagnetic surveys over mainland Greece has been put and presented together. At the same
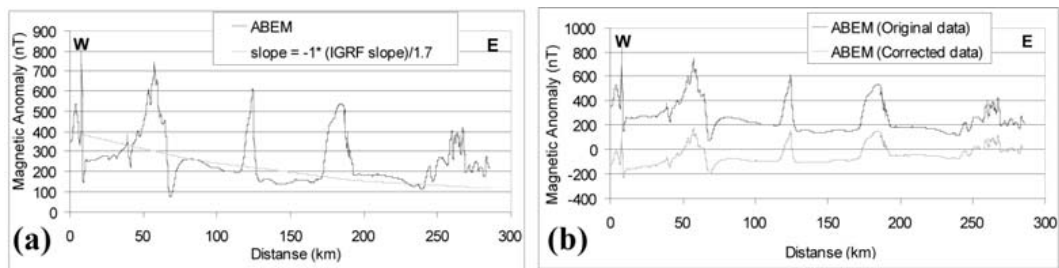
Fig. 5: (a) An E-W profile sliced from the ABEM data (Profile PB in Fig. 1). The trend line has been determined as per Fig. 3c. (b) The same profile before and after de-trending and re-scaling as per Fig. 3d.

time, it is very inhomogeneous and unusable for strategic planning and extended/ regional scale studies! In this form, it is only useful for the analysis of local or extended aeromagnetic anomalies limited to within areas of uniform data collection schemes (see Fig.1 and Section 2). Moreover, the ABEM data require additional processing (de-trending and re-scaling) in order to represent the true amplitudes of local aeromagnetic anomalies. The homogenization of the mosaic map of Fig. 4 leading to the construction of the first complete aeromagnetic map of mainland Greece is presented in the following Section 4.

4. Homogenization

As mentioned previously, by "homogenization" of the mosaic map of Fig. 4, we imply the reference of the entire map to a common and *unique* constant ground clearance, or to a *unique* elevation AMSL. This is an exercise in upward/ downward continuation with the added difficulty that the observation surface (flight altitude) is not flat – the aircraft flew at a constant clearance (height) above the ground surface, following the contours of the terrain. Thus, direct methods of up- or downward continuation assuming flat observation surfaces (e.g. Fourier-based) cannot be applied because the magnetic field intensity obeys an inverse square attenuation law. We need to apply continuation of the field between arbitrary surfaces and in such cases the method of choice is the method of equivalent sources.

We have chosen to use the highly accurate and computationally efficient approach described by Xia et al (1993). This is a two-stage procedure: The first step requires the computation of an equivalent source layer at a horizontal surface below the lowest elevation of the observation and continuation surfaces. The layer is in fact a grid of sources which is iteratively assigned with a distribution of magnetizations through forward calculation of the anomaly on the observation surface, so as to faithfully reproduce the observed total magnetic field. In a second step, the field is up- or downward continued to any arbitrary surface by forward computation on the basis of the equivalent source layer.

In our case, the exact observation surface (flight contour) is not known, but may be approximated to arbitrary precision on the basis of a digital elevation model (DEM). Herein, we have used a 100´100 m DEM based on the 1:50.000 scale maps of the HAGS. The DEM grid was re-interpolated to the nodes of the aeromagnetic grid and the appropriate adjustments were applied at each node, in order to reproduce the ground clearance parameters of the area at which the grid point belongs.

On the basis of the thusly approximated observation surface, the procedure of Xia et al (1993) was applied separately for each area described in Section 2 and the final "unified and homogeneous" aeromagnetic map was constructed by collating the mosaic of up- or downward continued grids, commonly referenced to a *unique* constant ground clearance, or to a *unique* elevation AMSL. Prior to upward continuation, the ABEM data was de-trended and re-scaled according to the procedure of
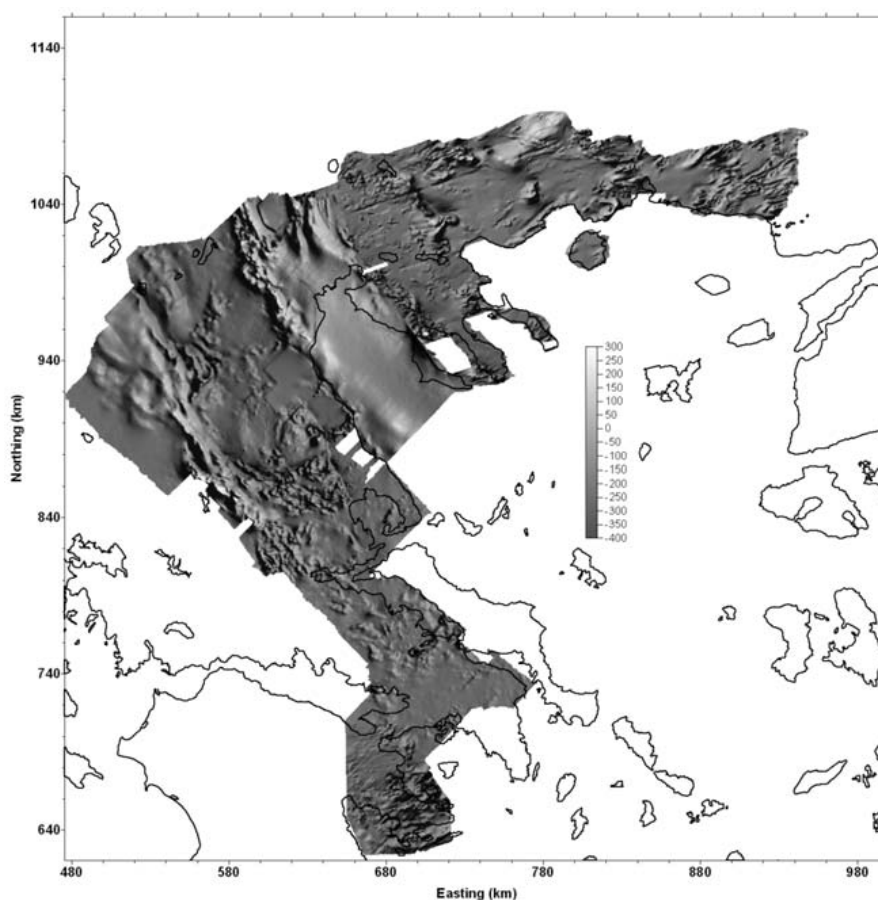
Fig. 6: The aeromagnetic map of the Hellenic mainland homogenized at 300 m AGL In this final product the ABEM data have been de-trended and re-scaled according to the discussion of Section 3. The map is presented in shaded relief form, lit from the NW.

Section 3, in order to correct for the distorted IGRF correction and the resulting grid was adopted only after demonstrating compliance with the Hunting and Turkish data.

Herein we present two versions of the unified and homogeneous map. Fig. 6 illustrates the map at a *constant ground clearance* of 300m AGL and Fig. 7 is the same, upward continued to a *constant altitude* of 3000m AMSL. Both maps are presented in the form of a shaded relief lit from the NW, in order to accentuate their respective characteristics and facilitate the brief discussion to be presented in Section 5.

5. Brief Discussion and Conclusions

The unified and homogeneous maps presented herein show for the first time, a complete and unified image of the crustal magnetic field at regional – national scale. In these images, the signatures of many isopic zones and rock formations comprising the Hellenic mainland are clearly seen, with particular reference to the ophiolite suites. Thus, a different and very interesting glimpse at the Alpine and post-alpine tectonics of the Hellenic territories is possible.

To begin with, the aeromagnetic data roughly delineate the boundaries of isopic zones, or groups of isopic zones. Thus, from east to west, the following groups of zones can (more or less) clearly be
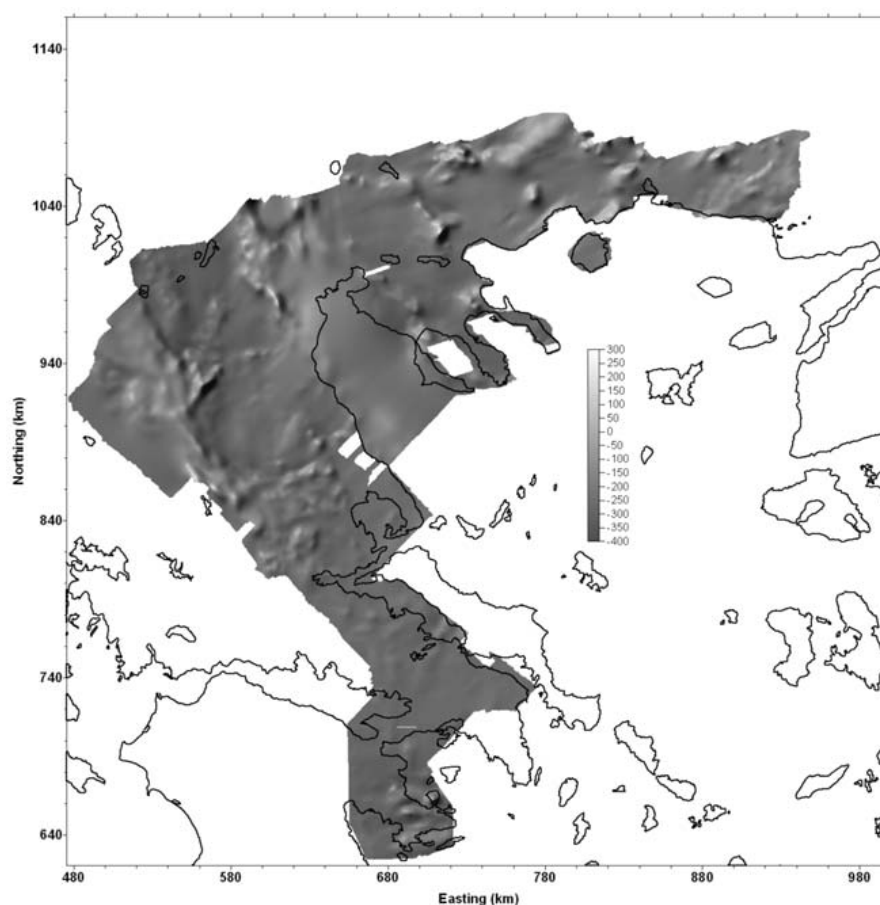
Fig. 7: The aeromagnetic map of the Hellenic mainland homogenized at 3000 m AMSL In this final product the ABEM data have been de-trended and re-scaled according to the discussion of Section 3. The map is presented in shaded relief form, lit from the NW.

defined: (a) The Rhodope massif; this can be distinguished from the Circum-Rhodope belt at the SE of Evros due to the remarkable roughness of the magnetic terrain observed there, presumably due to tectonism. (b) The Serbomacedonian massif; (c) the Circum-Rhodope and Peania zones; (d) the Paikon and Vardar zones; (e) the Pelagonian and Sub-Pelagonian zones.

These groups of zones are mainly differentiated (bounded) by the emplacement of intrusive rocks, especially at northern Greece and, mainly, the emplacement of ophiolite suites. Conversely, the Pindos and Gavrovo zones at the W-NW end of the map and glimpses of the Parnassus zone stand out because of the low to very low magnetizations of their associated stratigraphic sequences.

The magnetic signatures of the ophiolite sequences of the Pelagonian and Sub-pelagonian zones deserve some attention and will be briefly commented starting at the north. The magnetic signature of the Pindos ophiolites appears stronger than those of Vourinos, which according to Papanikolaou (2009) belong to the H4 Axios-Vardar terrane. This may suggest that the Vourinos and Pindos ophiolites do not link beneath the sediments of the Mesohellenic Trough, as proposed by Rassios et al. (1983) and Jones & Robertson (2001). A conspicuous, NE-SW anomaly is observed north of Kalambaka, marking, more or less, the northern boundary of Mt Antihasia. Quite interestingly, it lays on the SW-prolongation of the Aliakmon – Servia Fault Zone and also marks the southernmost bound-

ary of the Vourinos ophiolites.

An arcuate "trough" can be seen, passing east of Karditsa, marking the northern limit of Mt Phyllion and reaching close to the SW flanks of Mt Ossa. It separates the southern part of the Thesally basin from the northern one. Within the former, the Tertiary and Quaternary sedimentary cover appears to be considerably thinner, while the underlying alpine occurrences appear intensely dismembered and dissected by NW-SE, NE-SW and probably E-W tectonic contacts (faults). Actually this area appears to be also bounded on the east by a NNW-SSE discontinuity, the nature of which is at present enigmatic. A little further to the south, a practically straight, ENE-WSW discontinuity marks the southern margin of the Thessaly plain. It can be traced from the Nea Anchialos on the NW part of Pagasitikos Gulf to Domokos and it coincides with the Nea Anchialos Fault, which marks the northern boundary of the Almyros Basin (Caputo & Pavlides, 1993), locus of several earthquakes in the previous century (Papadimitriou & Karakostas, 2003). It is also noteworthy that this ENE-WSW discontinuity seems to change polarity, as at its eastern part (Almyros basin) it appears to be a steep, south-dipping fault, while in the west, the downthrown block is the northern one, corresponding to the Karditsa plain.

The area of eastern Central Greece (Sterea Hellas) is weaved with an intricate pattern of intermediate amplitude anomalies due to an ophiolite sequence dismembered and dissected mainly by NW-SE, NE-SW faulting. The nature of these features has recently been discussed by Tzanis et al (2010). Finally, the magnetic signatures of (Sub-pelagonian) rocks at the Argolis peninsula in central-eastern Peloponnesus is also quite rough, with prevailing E-W and NW-SE discontinuities, the nature of which is yet to be determined.

Returning to northern Greece, the signature of the Axios-Vardar ophiolites, as well as the boundaries of this ophiolite suture are clearly discernible, both inland and offshore, in the Thermaikos Gulf. The strong, indented anomaly on the western margin of the Strymon half-graben does not seem to correspond to the inferred fault that bounds the basin on the west, which develops on the hanging-wall of the Strymon Valley Detachment (Dinter, 1998). Instead it appears to be related to the boundary between the Vertiskos and Kerdyllia Units, (Papanikolaou, 1993). Another interesting observation is that the high-angle, NW-SE normal faults that bound the Strymon and Drama basins are not directly identifiable in the aeromagnetic map. Some tertiary intrusive bodies appear to have stronger magnetic signature than others. For example, the Vrondou pluton, north of Serrai, stands out very clearly, while the Symvolon granite, west of Kavala is less prominent. However, even in this latter case, its boundaries, which are related to the major Kavala-Xanthi-Komotini Fault (KXK), are seen as extended linear "troughs" oriented NE-SW and most probably correspond to the Symvolon Shear Zone, according to Dinter (1998). A structure of similar orientation (NE-SW) is also observed at the delta of Nestos River, parallel to the present-day coastline. This zone may also correspond to a sheared block, related to the KXK or a structure parallel to it. As a matter of fact, further to the east, in the Alexandroupolis- Evros area, several NE-SW to ENE-WSW lineations, most probably related to faults with predominant strike-slip character, can be observed. A high-intensity 'islet' is located at the south-eastern part of the Drama supradetachment half-graben. This feature may be related to a buried intrusive body, related to the Symvolon granite, which has been cut off and displaced by the combined activity of the KXK and the Drama Faults (see Stampolidis and Tsokas, 2004 for additional information). Between Xanthi and Porto Lago, the observed high magnetic values may equally be related to buried intrusive bodies; this, in turn, can be associated with the Nea Kessani geothermal field (Kolios et al., 2005). It is also worth noting that while many linear features can be directly associated with faulting as discussed above, others may not be as easily explainable. A prime example is the long NE-SW lineament parallel to the Greek-Bulgaria border along the line Mavrovouni – Falakron – West Rhodope Mts., whose nature is at present a mystery!

To conclude our brief presentation, we note that herein we have presented the first regional – national scale digital maps of homogeneous aeromagnetic data at different reference surfaces. As shown in the brief discussion above, these maps offer the opportunity to conduct studies of regional or spatially extended aeromagnetic anomalies, as well as local, kilometric scale anomalies; this was hitherto not feasible with the existing inhomogeneous, printed 1:50000 scale map series. Inasmuch as the aeromagnetic maps are principally used for the analysis of extended – regional scale features and strategic planning, the new set of maps contribute an important piece of geo-scientific infrastructure and the opportunity to utilize a valuable resource for pure and applied geophysical and geological research.

6. Acknowledgements

7. References

ABEM, 1967, Final Report on an Airborne Geophysical Survey carried out for the Greek Institute for Geology and Subsurface Research during the year 1966 by ABEM-AB Elektrisk Malmletning, Stockholm

Akin, U., 2007. Aeromagnetic Map (Total Intensity) of Turkey, General Directorate of Mineral Research and Exploration, Ankara, Turkey

Caputo, R. & Pavlides, S., 1993. Late Cainozoic geodynamic evolution of Thessaly and surroundings (central-northern Greece). *Tectonophysics*, 223, 339-362.

Dinter, D., 1998. Late Cainozoic extension of the Alpine collisional orogen, north-eastern Greece: Origin of the north Aegean basin. *Bull. Geol. Soc. America*, 110, 1208-1230.

Jones, G., Robertson, A.H.F., 1991. Tectono-stratigraphy and evolution of the Mesozoic Pindos Ophiolite and related units, Northwestern Greece., *J. Geol. Soc. London* 148, 267– 288.

Kolios, N., Koutsinos, S., Arvanitis, A., Karydakis, G., 2005. Geothermal Situation in North-eastern Greece, Proc. World Geothermal Congress Antalya, Turkey, 24-29 April 2005, 1-14.

Papadimitriou, E. & Karakostas, V, 2003. Episodic occurrence of strong (M_wv6.2) earthquakes in Thessalia area (central Greece). *Earth Plan. Sci. Let.*, 215, 395-409.

Papanikolaou, D., 1993. Geotectonic evolution of the Aegean. Proc. 6th Congress of the Geological Society of Greece, *Bull. Geol. Soc. Greece*, 28/1, 33–48.

Papanikolaou, D., 2009. Timing of tectonic emplacement of the ophiolites and terrane paleogeography in the Hellenides. *Lithos*, 108, 262-280.

Rassios, A., Beccaluva, L., Bortolotti, V., Moores, E.M., 1983. The Vourinos ophiolite complex. *Ofioliti* 8, 275– 292.

Stampolidis, A., 1999. The Geomagnetic field in Macedonia and Thrace and its relationship with the geophysical and geological structure of the area, Doctoral Dissertation, Aristotelian University of Thessaloniki, 258pp (in Greek).

Stampolidis, A. and Tsokas G., 2004. Location of magnetic contacts and depth estimates for the magnetic sources from the aeromagnetic data of Macedonia and Thrace, Proceedings of the 10th Int. Congress, Thessaloniki, April 2004, in *Bull. Geol. Soc. Greece*, vol. XXXVI, 1252 – 1261 (in Greek).

Tzanis, A., Kranis, H. and Chailas, S., 2010. An investigation of the active tectonics in central-eastern mainland Greece, with imaging and decomposition of topographic and aeromagnetic data. *J. Geodyn.*, 49, 55 – 67 (doi:10.1016/j.jog.2009.09.042).

Xia, J., Sprowl, D.R. and Adkins-Heljeson, D., 1993. Correction of topographic distortions in potential-field data: A fast and accurate approach; *Geophysics*, 58(4), 515-523